



## Summertime ENSO–North African–Asian Jet teleconnection and implications for the Indian monsoons

Jeffrey Shaman<sup>1</sup> and Eli Tziperman<sup>2</sup>

Received 19 December 2006; revised 13 April 2007; accepted 14 May 2007; published 12 June 2007.

[1] Recent findings indicate that ENSO may modulate the strength of the Indian monsoons by altering the meridional tropospheric temperature gradient between Asia and the equatorial Indian Ocean. Here we show that during northern hemisphere summertime El Niño events both colder upper tropospheric temperatures and increased vorticity anomalies are observed within the North African–Asian (NAA) jet. The temperature response within the NAA jet is the dominant ENSO-related change to the meridional tropospheric temperature gradient between Asia and the equatorial Indian Ocean. Forced solutions of the linearized barotropic vorticity equation indicate that these anomalies within the NAA jet are a response to northern hemisphere summertime El Niño-related convective activity over the equatorial Pacific Ocean. Additional experiments indicate that westward propagating anomalies in both the tropics and middle latitudes produce the anomaly response within the NAA jet. These findings suggest that the teleconnection linking ENSO and the monsoons is mediated by the response of the NAA jet to westward propagating Rossby waves. **Citation:** Shaman, J., and E. Tziperman (2007), Summertime ENSO–North African–Asian Jet teleconnection and implications for the Indian monsoons, *Geophys. Res. Lett.*, *34*, L11702, doi:10.1029/2006GL029143.

### 1. Introduction

[2] The significant summertime covariability of the Indian monsoons and ENSO has been documented in numerous studies [Walker, 1924; Rasmusson and Carpenter, 1983; Ropelewski and Halpert, 1987; Webster and Yang, 1992; Mehta and Lau, 1997; Webster *et al.*, 1998]. This covariability generally manifests as a weaker Indian monsoon during summertime El Niño events. Some evidence exists suggesting that this relationship between ENSO and the Indian monsoons fluctuates on decadal timescales and may have deteriorated in the late 20th century [Kumar *et al.*, 1999; Krishnamurthy and Goswami, 2000; Ashrit *et al.*, 2001]; however, more recent findings indicate that these fluctuations may be merely a stochastic process and not statistically significant [Gershunov *et al.*, 2001; Van Oldenborgh and Burgers, 2005]. In addition, Goswami and Xavier [2005] showed that ENSO–Indian covariability depends in part on how the monsoon season is

defined and that the association between ENSO and Indian monsoon rainfall, in fact, has remained significant.

[3] A number of competing theories attempt to explain the observed covariability of the Indian monsoons and ENSO (see Auxiliary Material<sup>1</sup>). Recently, a new theory explaining this covariability was presented by Goswami and Xavier [2005]; these authors showed that summertime ENSO conditions are associated with tropospheric temperature anomalies over Asia and the Indian Ocean. Specifically, during summertime El Niño events anomalously cold temperatures occur over much of Asia and warm temperatures occur over the Indian Ocean. Such changes in the meridional gradient of tropospheric temperatures can affect monsoon circulation [Webster *et al.*, 1998]. Previous research has demonstrated that the onset of the South Asian monsoons is associated with both the upper tropospheric temperature gradient between the Himalayas and the Indian Ocean [He *et al.*, 1987, 2003; Li and Yanai, 1996] and the summertime heating of the Tibetan Plateau [Luo and Yanai, 1984; Yanai *et al.*, 1992; Yanai and Li, 1994]. Li and Yanai [1996] also showed that the intensity of the Asian summer monsoons, as measured by an index of vertical shear, was associated with the upper tropospheric meridional temperature gradient between Asia and the equatorial Indian Ocean. Goswami and Xavier [2005] provide evidence that changes in the meridional tropospheric temperature gradient can also influence monsoon withdrawal and the overall length of the monsoon season.

[4] Over the Indian subcontinent, the meridional gradient of tropospheric temperature switches sign seasonally [He *et al.*, 2003]. In the summer, this meridional temperature gradient (i.e. hotter temperatures over Asia and colder temperatures over the Indian Ocean) through the thermal wind balance produces zonal winds with easterly vertical shear. This shear can be defined as the difference of the zonal winds at 200mb and 850mb over the Indian monsoon region and is often used as an index measure of the strength of the monsoons [Webster and Yang, 1992; Li and Yanai, 1996; He *et al.*, 2003; Goswami and Xavier, 2005].

[5] On an intraseasonal basis, the Indian monsoons have been characterized as the northward migration of Tropical Convergence Zone (TCZ) convection from the equatorial Indian Ocean to the Indian subcontinent [Sikka and Gadgil, 1980; Gadgil, 2003]. The rate of TCZ northward migration has been shown to be proportional to the magnitude of the easterly vertical shear of the zonal winds [Jiang *et al.*, 2004]. Seasonal anomalies in the meridional gradient of tropospheric temperatures can therefore modulate Indian monsoon rainfall by altering the easterly vertical shear of

<sup>1</sup>College of Oceanic and Atmospheric Sciences, Oregon State University, Corvallis, Oregon, USA.

<sup>2</sup>Department of Earth and Planetary Sciences and Division of Engineering and Applied Sciences, Harvard University, Cambridge, Massachusetts, USA.

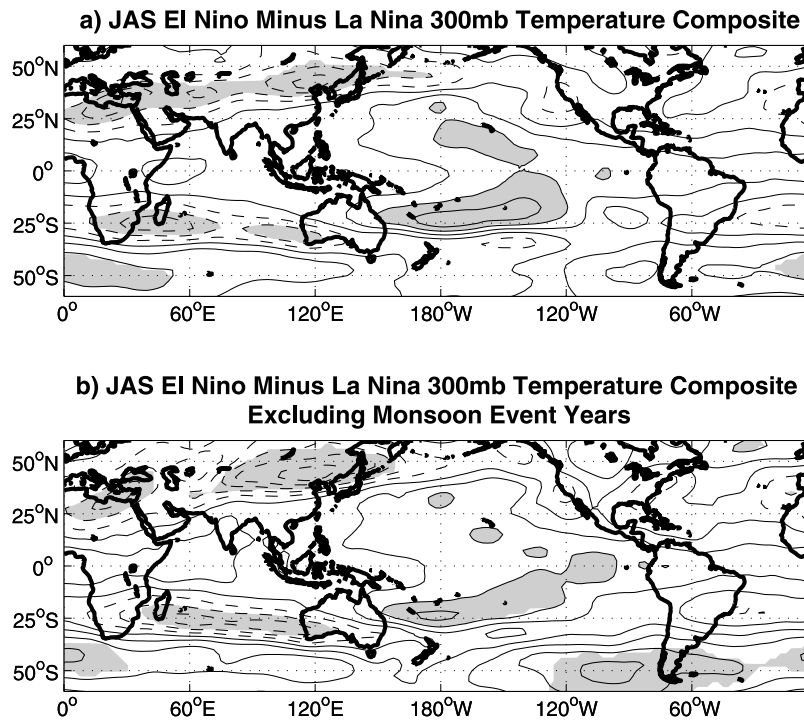


**Figure 1.** (a) Composite map of northern hemisphere summer (JAS) 300mb temperature anomalies based on JAS El Niño minus La Niña event years, using the NINO3 record ( $\pm 1$  std). El Niño event years are 1951, 1957, 1963, 1965, 1972, 1976, 1982, 1983, 1987, 1991 and 1997; La Niña event years are 1949, 1954, 1964, 1970, 1973, 1975, 1988 and 1999. Contour interval is 0.5K. Negative contours are dashed. Shaded areas are significant ( $p < 0.05$ ) based on bootstrap confidence intervals estimated by generation of 5000 random composite maps from the 1949–2006 JAS NCEP-NCAR reanalysis record. (b) As in Figure 1a but excluding JAS El Niño event years with weak Indian monsoon rainfall ( $\leq -1$  standard deviation of JJAS All-India rainfall) and excluding La Niña event years with strong Indian monsoon rainfall ( $\geq -1$  standard deviation of JJAS All-India rainfall). El Niño event years without weak Indian monsoon rainfall are 1957, 1963, 1976, 1983, 1991 and 1997; La Niña event years are 1949, 1954, 1964, 1973 and 1999.

the zonal winds, which in turn change the northward migration rate of the TCZ and thus the number of intraseasonal storm systems reaching India in a monsoon season. A weakening of the meridional gradient of upper tropospheric temperatures will thus reduce the easterly vertical shear of the zonal winds and reduce monsoon rainfall.

[6] In this paper we characterize the association of temperature anomalies over Asia with ENSO variability and show that these temperature anomalies are linked with vorticity changes in the North African-Asian (NAA) jet. This linkage naturally leads to an investigation of the vorticity changes within the NAA jet induced by ENSO. Our findings indicate that westward propagating stationary barotropic Rossby waves in both the tropics and mid-latitudes produce the vorticity and temperature anomalies in the NAA jet, which in turn affect the Indian monsoons.

## 2. Data

[7] The sea surface temperature averaged over the NINO3 region (5N–5S, 150W–90W) was the index of ENSO used for this study [Kaplan *et al.*, 1998]. NCEP-NCAR Reanalysis Project monthly global fields for July–September (JAS) 1949–2006 were used as well [Kalnay *et al.*, 1996]. Three sets of distributed rainfall data

for 1979–2006 were employed in this study: 1) Climate Anomaly Monitoring System Outgoing longwave radiation Precipitation Index (CAMS OPI) estimates; 2) National Oceanic and Atmospheric Administration (NOAA) Climate Prediction Center Merged Analysis of Precipitation (CMAP) using rain gauge, satellite estimates and numerical model predictions; 3) National Aeronautic and Space Administration (NASA) multi-satellite estimates of rainfall. Summer Indian monsoon rainfall was derived from All-India monthly rainfall data of the Indian Institute of Tropical Meteorology.

## 3. ENSO-Related Variability in the NAA Jet

[8] Composite maps of NCEP/NCAR reanalysis for summertime El Niño minus La Niña event years reveal significant temperature anomalies in the upper troposphere (Figure 1a). The strongest temperature anomalies lie along the core of the NAA jet. Similar anomalies are found at 200mb, 500mb and at the tropopause (see Figure S1). These cold temperatures within the NAA jet combined with a slight warming over the tropical Indian Ocean produce a 2–3K reduction of the meridional gradient of upper tropospheric temperatures. Composite maps show that monsoon rainfall is also associated with similar temperature changes (Figure S2). This finding is not unexpected as monsoon rainfall and ENSO variability are themselves

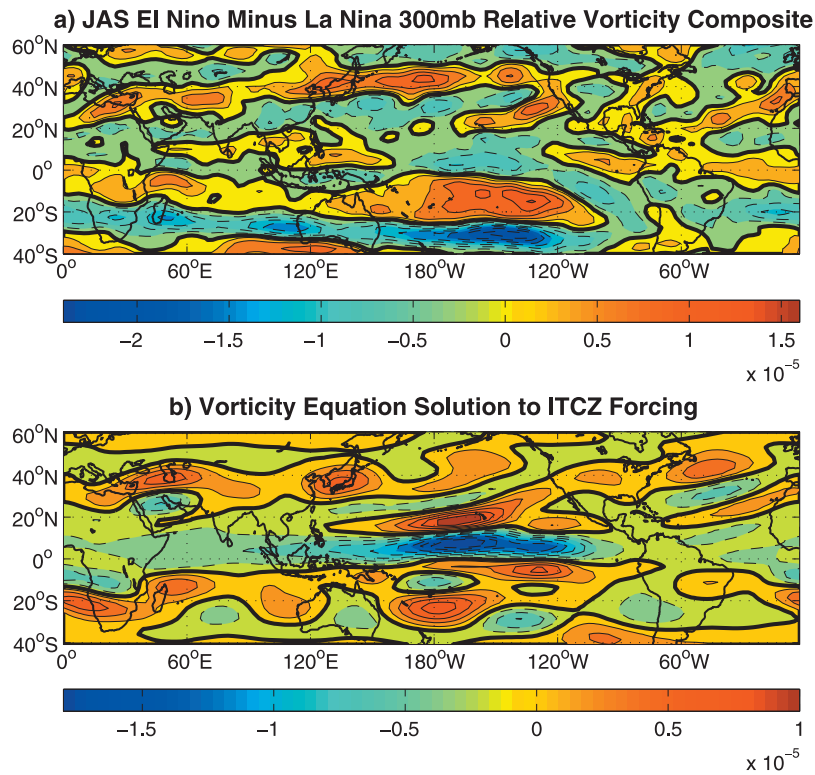


**Figure 2.** (a) Composite map of 300 mb vorticity based on El Niño minus La Niña event years, using the NINO3 record ( $\pm 1$ std). El Niño and La Niña event years are as in Figure 1a. Contour interval is  $3 \times 10^{-6} \text{ s}^{-1}$ . (b) Vorticity response of the barotropic vorticity equation linearized about the time-mean 1949–2006 JAS 300mb streamfunction to a forcing at 160–280°E, 0–10°N as specified in equation (2). Contour interval is  $2 \times 10^{-6} \text{ s}^{-1}$ . Negative contours are dashed and the zero contour is thickened in both plots.

correlated. In addition, similar temperature anomalies also exist in composite maps of summertime El Niño minus La Niña event years in which El Niño years coincident with a weak Indian monsoon and La Niña years coincident with a strong Indian monsoon are excluded (Figure 1b). This last composite map indicates that the temperature anomalies within the NAA jet may be tied to ENSO variability and not Indian monsoon variability.

[9] The NAA jet is a dominant feature of the upper troposphere. This jet is delineated by a zonal wind maximum that extends from the subtropical Atlantic Ocean across North Africa and South Asia to the North Pacific (Figure S3a). This upper tropospheric wind feature is observed in all seasons, though it manifests at higher latitudes during northern hemisphere summer.

[10] The zonal wind maximum at the NAA jet core produces a strong meridional gradient of absolute vorticity along the length of the jet (Figure S3b). According to Rossby wave theory, this maximum in the meridional gradient of absolute vorticity produces barotropic Rossby wave refraction, or bending, toward the jet core [Hoskins and Ambrizzi, 1993]. In addition, the NAA jet is flanked by minima in the meridional gradient of absolute vorticity to the north and south. These minima act as refractive barriers against most northward and southward Rossby wave propagation. As a consequence, Rossby wave energy cannot escape nor enter the NAA jet except at its mouth over the

subtropical Atlantic Ocean and at its tail over the north Pacific Ocean. Rossby waves that do enter the NAA jet propagate along the jet core. Such low-frequency energy trapped in the NAA jet has been associated with changes in stormtracks and precipitation within the jet [Branstator, 2002].

[11] Recent research has also shown that the NAA jet is part of a larger circumglobal pattern of northern hemisphere atmospheric covariability [Branstator, 2002; Watanabe, 2004; Ding and Wang, 2005]. In this paper, however, we will not be focusing on this covariability, but instead the response of the NAA jet to tropical forcing, specifically convective activity over the equatorial Pacific Ocean associated with northern hemisphere summertime El Niño conditions.

[12] Composite maps of relative vorticity for summertime El Niño minus La Niña event years also reveal positive anomalies along the length of the NAA jet (Figure 2a). This finding is not unexpected as cold potential temperature anomalies at the tropopause are dynamically equivalent to positive anomalies of pseudopotential vorticity in the upper troposphere [Bretherton, 1966], and increases in upper tropospheric potential vorticity tend to be coincident with a cooling of the upper troposphere [Hoskins et al., 1985]. In this context, it is apparent that the temperature anomalies observed in the NAA jet (Figure 1), and therefore the change in the upper tropospheric meridional temperature

gradient between Asia and the equatorial Indian Ocean, develop in concert with the vorticity changes observed in Figure 2a. We next show that the vorticity changes in the NAA jet are brought about by an atmospheric Rossby wave teleconnection with ENSO.

#### 4. Teleconnection Mechanism

[13] Given the potential role of vorticity and Rossby waves in creating the changes in NAA jet vorticity (Figure 2a) and in the upper tropospheric meridional temperature gradient between Asia and the equatorial Indian Ocean (Figure 1), we explore the ENSO-NAA jet teleconnection using a simplified model of the atmosphere. Forced solutions of the linearized barotropic vorticity equation were found following the solution method of *Branstator* [1983]. The barotropic vorticity equation was first linearized about a lowpass filtered (zonal wavenumbers 0–8) 300mb 1949–2006 climatology of NCEP-NCAR reanalysis July–September streamfunction. The equation to be solved is then

$$J(\bar{\psi}, \nabla^2 \psi') + J(\psi', \nabla^2 \bar{\psi} + f) + \alpha \nabla^2 \psi' + K \nabla^4 \nabla^2 \psi' = R \quad (1)$$

where  $\psi$  is the streamfunction,  $f$  is the Coriolis force,  $\alpha$  is the Rayleigh coefficient,  $K$  is a diffusion coefficient,  $R$  is a forcing function,

$$J(A, B) = \frac{1}{r^2} \left( \frac{\partial A}{\partial \lambda} \frac{\partial B}{\partial \mu} - \frac{\partial A}{\partial \mu} \frac{\partial B}{\partial \lambda} \right)$$

is the Jacobian,  $\lambda$  is longitude,  $\mu = \sin(\phi)$ ,  $\phi$  is latitude, and  $r$  is the earth's radius. Here the overbars indicate the seasonal time-mean flow (the basic state); primes signify the perturbation flow to be solved.  $\alpha$  was set to  $1.57 \times 10^{-6} \text{ s}^{-1}$  (an e-folding time of 1/(7 days)), and  $K$  was set to  $2.34 \times 10^{16} \text{ m}^4 \text{ s}^{-1}$ . The anomaly forcing was specified as

$$R = -(f + \nabla^2 \bar{\psi})D \quad (2)$$

where  $D$ , forcing divergence, is set to  $3 \times 10^{-6} \text{ s}^{-1}$ . Equation (1) was solved using spherical harmonics and triangular 24 truncation (T24) (see *Branstator* [1983] for solution method details).

[14] During northern hemisphere summertime El Niño events, precipitation increases throughout the equatorial Pacific (Figure S4). West of 150°W, the rainfall anomalies straddle the equator. However, much of the precipitation, including the strongest northern hemisphere rainfall anomalies, occurs along the Intertropical Convergence Zone (ITCZ) from about 160°E–80°W between the equator and 10°N. Figure 2b presents the solution of the linearized barotropic vorticity equation in response to forcing divergence along the ITCZ (see Figure S5 for forcing structure). The vorticity solution produces positive vorticity anomalies within the NAA jet similar to the positive vorticity anomalies observed in the reanalysis composite for northern hemisphere summertime El Niño minus La Niña event years (Figure 2a). This vorticity solution is insensitive to the size and shape of the forcing along the ITCZ (see Figure S6 and its description). These findings

indicate that the anomalies in the NAA jet could be a response to northern hemisphere summertime El Niño-related convection along the ITCZ over the equatorial Pacific Ocean, and that stationary barotropic Rossby waves produce this teleconnection.

[15] In the temperature and relative vorticity composites presented here for northern hemisphere summertime El Niño minus La Niña event years (Figures 1 and 2a), there is no clear atmospheric wave train emanating from above the equatorial Pacific Ocean. The solution of the barotropic vorticity equation linearized about northern hemisphere summertime climatology and forced with divergence along the ITCZ also fails to produce a clear wave path (Figure 2b). To determine how the El Niño response vorticity anomalies arrive at the NAA jet, we added areas of high damping (sponge layers) to different regions of the atmosphere while solving the linearized barotropic vorticity equation. Bands of friction to the west of the ITCZ forcing region eliminated the vorticity response within the NAA jet, whereas friction to the east of the ITCZ forcing region had no effect on the vorticity response within the NAA jet (Figure 3).

[16] These findings indicate that a westward propagating atmospheric signal links the vorticity and temperature anomalies in the NAA jet to convective activity over the equatorial Pacific Ocean. These vorticity disturbances are produced by stationary barotropic Rossby wave energy, which propagates at the group velocity and can be derived explicitly from the dispersion relation of the inviscid form of equation (1) [*Karoly*, 1983]. Whereas a zonally symmetric background would admit only eastward stationary barotropic Rossby wave propagation [*Hoskins and Karoly*, 1981], westward stationary barotropic Rossby wave propagation can occur within the more realistic zonally asymmetric background used here [*Karoly*, 1983].

[17] More specifically, it was found that damping to the west of the ITCZ forcing anywhere between the equator and 40°N would disrupt the response in the NAA jet. For instance at 150°E, damping from 0–10°N, 0–20°N, 0–30°N and finally 0–40°N is progressively more disruptive of the response in the NAA jet (Figures S7 and S8). These results suggest that barotropic Rossby waves that originate from the area of the ITCZ and propagate both directly westward, as well as via the mid latitudes, toward the NAA may be important for creating the response within the NAA jet.

#### 5. Discussion

[18] The findings presented here show that the upper tropospheric meridional temperature gradient between Asia and the equatorial Indian Ocean responds to northern hemisphere summertime ENSO variability. Most of this upper tropospheric temperature sensitivity resides within the NAA jet, where temperature changes are dynamically linked with changes in vorticity. Our findings with a simple linear model of the upper troposphere indicate that the NAA jet responds to the upper tropospheric divergence over the equatorial Pacific Ocean, which is associated with northern hemisphere summertime El Niño-related convective anomalies. This atmospheric teleconnection appears to be mediated by a westward propagating signal from the Pacific basin to the NAA jet and Indian Ocean basin.

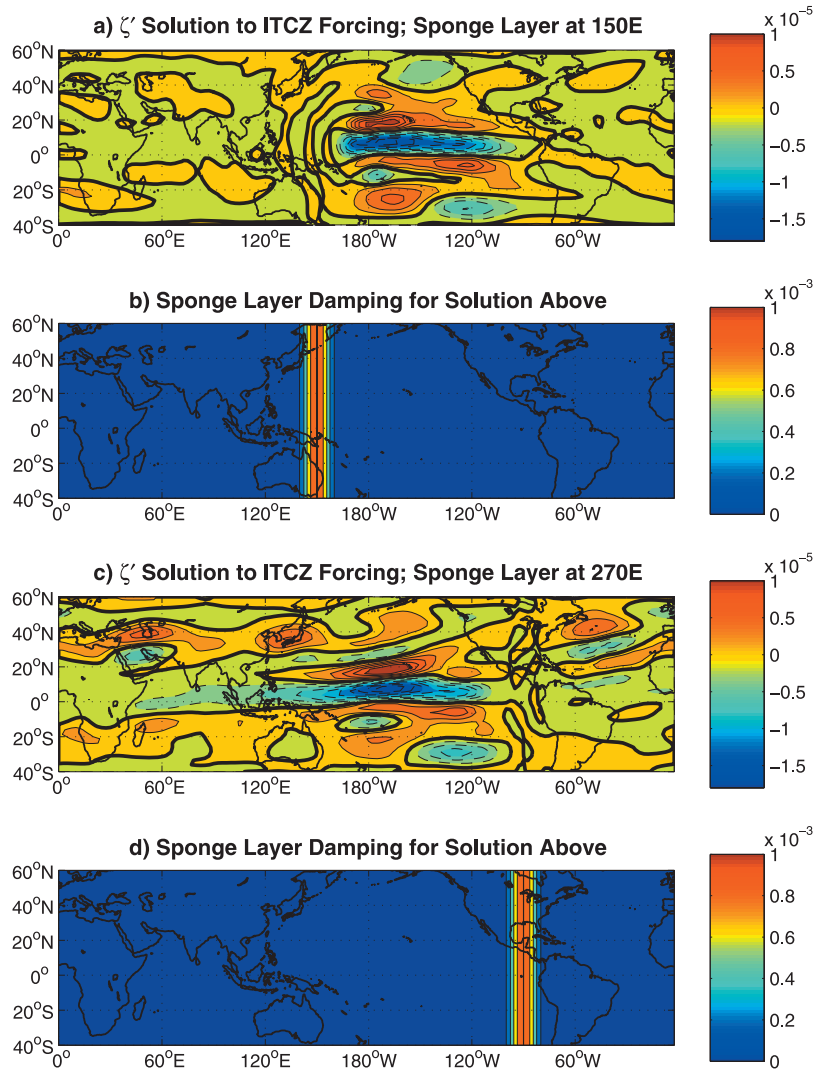


**Figure 3.** (a) Vorticity response of the barotropic vorticity equation linearized about the time-mean 1949–2006 JAS 300mb streamfunction to a forcing at  $160\text{--}280^\circ\text{E}$ ,  $0\text{--}10^\circ\text{N}$  with a sponge layer of high damping extending pole-to-pole and centered at  $150^\circ\text{E}$ . Contour interval is  $2 \times 10^{-6}\text{s}^{-1}$ . Negative contours are dashed and the zero contour is thickened. (b) Sponge layer damping used in the solution to Figure 3a. Contour interval is  $2 \times 10^{-4}\text{s}^{-1}$ . (c) As for Figure 3a but with damping centered at  $270^\circ\text{E}$ . (d) As for Figure 3b.

[19] These findings highlight a possible role for the NAA jet in determining the seasonal strength of the Indian monsoons. The teleconnection begins with convective anomalies along the ITCZ over the equatorial Pacific Ocean that are produced during northern hemisphere summertime El Niño events. These convective anomalies generate divergence in the upper troposphere and westward propagating vorticity disturbances. These westward propagating Rossby waves manifest as positive vorticity anomalies along the length of the NAA jet. Cold temperature anomalies also develop in association with these positive vorticity anomalies [Hoskins *et al.*, 1985]. The cold temperature anomalies within the NAA jet reduce the upper tropospheric meridional temperature gradient between Asia and the equatorial Indian Ocean. This change in the temperature gradient alters the thermal wind balance and reduces the easterly vertical shear of the zonal winds. The

reduced easterly vertical shear of the zonal winds slows northward TCZ migration to the Indian subcontinent [Jiang *et al.*, 2004], and thus decreases the number of intraseasonal storm systems reaching land within a monsoon season. With fewer intraseasonal storm systems reaching the Indian subcontinent, seasonal monsoon rainfall is reduced.

[20] A number of details of the northern hemisphere summertime ENSO-NAA jet teleconnection remain to be described. Our findings indicate that the NAA jet may respond to ENSO convective activity in linear, barotropic fashion. However, future investigations of this teleconnection, which take into account other possible effects, are warranted. For instance, the use of linear dynamics ignores possible nonlinear transient eddy amplification effects. In addition, within the NAA jet, wave-mean flow interaction and energy conversion [Li and Nathan, 1997], and baroclinic effects, such as vertical advection and twisting

[Sardeshmukh and Hoskins, 1988], may also modify the atmospheric response. Future examinations of the proposed teleconnection to the NAA jet should include these nonlinear and baroclinic dynamics. In addition, in the northern hemisphere *winter*, evidence for an eastward propagating teleconnection from the Pacific to the NAA jet has been found [Shaman and Tziperman, 2005]. No such eastward signal has been identified here for the summer. These seasonal differences need to be explored.

[21] Recent work indicates that Indian monsoon sensitivity to ENSO may depend on both the magnitude and location of SST anomalies in the equatorial Pacific Ocean [Kumar et al., 2006]. This work found that the Indian monsoons appear more sensitive to northern hemisphere summertime warming of the central equatorial Pacific Ocean. The sensitivities of the NAA jet to ENSO should be further explored in this context.

[22] The ENSO-related anomalies within the NAA jet may also affect other regional climate and weather systems. Conversely, other climate features may modulate conditions in the NAA jet. For instance, interannual changes in Eurasian land surface temperatures could conceivably change the temperature of the overlying atmosphere. In particular, land surface temperature changes due to snowpack variability on the Tibetan Plateau would likely change temperatures in the NAA jet. Monsoon convection itself may also feed back on the NAA jet via Rossby waves [e.g., Rodwell and Hoskins, 2001]. Further investigation of these potential influences is warranted. The sub-seasonal variability of NAA jet temperature anomalies also needs to be studied further; such variability may have important implications for the timing of monsoon onset and withdrawal, as shown by Goswami and Xavier [2005], as well as break activity. In addition, the sub-seasonal variability of land and sea surface temperatures may modulate the response of the monsoons to the NAA jet and upper tropospheric meridional temperature gradient anomalies.

[23] At its strongest during the 20th century, the correlation of ENSO and the Indian monsoons explained ~25% of Indian monsoon rainfall variance [Kumar et al., 1999]. Clearly, other factors, such as Tibetan Plateau snowpack, the Madden-Julian Oscillation, and Indian Ocean dynamics, may also be affecting Indian monsoon interannual variability. However, a further understanding of the ENSO-NAA jet teleconnection may help improve dynamical prediction of the Indian monsoons.

[24] **Acknowledgments.** This research was supported by the McDonnell Foundation and by the NSF Climate Dynamics program, grant ATM 0351123. We thank G. Branstator, M. Brenner, I. Eisenman, K. Emanuel, B. Farrell and N. Hamik for helpful discussions.

## References

- Ashrit, R. G., K. R. Kumar, and K. K. Kumar (2001), ENSO-monsoon relationships in a greenhouse warming scenario, *Geophys. Res. Lett.*, **28**, 1727–1730.
- Branstator, G. (1983), Horizontal energy propagation in a barotropic atmosphere with meridional and zonal structure, *J. Atmos. Sci.*, **40**, 1689–1708.
- Branstator, G. (2002), Circumglobal teleconnections, the jet stream waveguide, and the North Atlantic oscillation, *J. Clim.*, **15**, 1893–1910.
- Bretherton, F. P. (1966), Critical layer instability in baroclinic flows, *Q. J. R. Meteorol. Soc.*, **92**, 325–334.
- Ding, Q. H., and B. Wang (2005), Circumglobal teleconnection in the Northern Hemisphere summer, *J. Clim.*, **18**, 3483–3505.
- Gadgil, S. (2003), The Indian monsoon and its variability, *Annu. Rev. Earth Planet. Sci.*, **31**, 429–467.
- Gershunov, A., N. Schneider, and T. Barnett (2001), Low-frequency modulation of the ENSO-Indian monsoon rainfall relationship: Signal or noise?, *J. Clim.*, **14**, 2486–2492.
- Goswami, B. N., and P. K. Xavier (2005), ENSO control on the south Asian monsoon through the length of the rainy season, *Geophys. Res. Lett.*, **32**, L18717, doi:10.1029/2005GL023216.
- He, H., J. W. McGinnis, Z. Song, and M. Yanai (1987), Onset of the Asian monsoon in 1979 and the effect of the Tibetan Plateau, *Mon. Weather Rev.*, **115**, 1966–1995.
- He, H., C.-H. Sui, M. Jian, Z. Wen, and G. Lan (2003), The evolution of tropospheric temperature field and its relationship with the onset of Asian summer monsoon, *J. Meteorol. Soc. Jpn.*, **81**, 1201–1223.
- Hoskins, B. J., and T. Ambrizzi (1993), Rossby wave propagation on a realistic longitudinally varying flow, *J. Atmos. Sci.*, **50**, 1661–1671.
- Hoskins, B. J., and D. J. Karoly (1981), The steady linear response of a spherical atmosphere to thermal and orographic forcing, *J. Atmos. Sci.*, **38**, 1179–1196.
- Hoskins, B. J., M. E. McIntyre, and A. W. Robertson (1985), On the use and significance of isentropic potential vorticity maps, *Q. J. R. Meteorol. Soc.*, **111**, 877–947.
- Jiang, X., T. Li, and B. Wang (2004), Structures and mechanisms of the northward propagation of the boreal summer intraseasonal oscillation, *J. Clim.*, **17**, 1022–1039.
- Kalnay, E., et al. (1996), NCEP/NCAR 40-year reanalysis project, *Bull. Am. Meteorol. Soc.*, **77**, 437–471.
- Kaplan, A., M. Cane, Y. Kushnir, A. Clement, B. Blumenthal, and B. Rajagopalan (1998), Analyses of Global Sea Surface Temperature 1856–1991, *J. Geophys. Res.*, **103**, 18,567–18,589.
- Karoly, D. J. (1983), Rossby-wave propagation in a barotropic atmosphere, *Dyn. Atmos. Oceans*, **7**, 111–125.
- Krishnamurthy, V., and B. N. Goswami (2000), Indian monsoon-ENSO relationship on interdecadal timescale, *J. Clim.*, **13**, 579–595.
- Kumar, K. K., B. Rajagopalan, and M. A. Cane (1999), On the weakening relationship between the Indian monsoon and ENSO, *Science*, **284**, 2156–2159.
- Kumar, K. K., B. Rajagopalan, M. Hoerling, G. Bates, and M. A. Cane (2006), Unraveling the mystery of Indian monsoon failure during El Niño, *Science*, **314**, 115–119.
- Li, C., and M. Yanai (1996), The onset and interannual variability of the Asian summer monsoon in relation to land-sea-thermal contrast, *J. Clim.*, **9**, 358–375.
- Li, L., and T. R. Nathan (1997), Effects of low-frequency tropical forcing on intraseasonal tropical-extratropical interactions, *J. Atmos. Sci.*, **54**, 332–346.
- Luo, H., and M. Yanai (1984), The large-scale circulation and heat sources over the Tibetan Plateau and surrounding areas during the early summer of 1979. Part II: Heat and moisture budgets, *Mon. Weather Rev.*, **112**, 966–989.
- Mehta, V. M., and K.-M. Lau (1997), Influence of solar irradiance on the Indian monsoon-ENSO relationship at decadal-multidecadal time scales, *Geophys. Res. Lett.*, **24**, 159–162.
- Rasmusson, E. M., and T. H. Carpenter (1983), The relationship between eastern equatorial Pacific sea-surface temperatures and rainfall over India and Sri Lanka, *Mon. Weather Rev.*, **111**, 517–528.
- Rodwell, M. J., and B. J. Hoskins (2001), Subtropical anticyclones and summer monsoons, *J. Clim.*, **14**, 3192–3211.
- Ropelewski, C. F., and M. S. Halpert (1987), Global and regional scale precipitation patterns associated with the El Niño/Southern Oscillation, *Mon. Weather Rev.*, **115**, 1606–1626.
- Sardeshmukh, P. D., and B. J. Hoskins (1988), The generation of global rotational flow by steady idealized tropical divergence, *J. Atmos. Sci.*, **45**, 1228–1251.
- Shaman, J., and E. Tziperman (2005), The effect of ENSO on Tibetan Plateau snow depth and the South Asian monsoons: a stationary wave teleconnection mechanism, *J. Clim.*, **18**, 2067–2079.
- Sikka, D. R., and S. Gadgil (1980), On the maximum cloud zone and the ITCZ over Indian longitudes during the southwest monsoon, *Mon. Weather Rev.*, **108**, 1840–1853.
- Van Oldenborgh, G. J., and G. Burgers (2005), Searching for decadal variations in ENSO precipitation teleconnections, *Geophys. Res. Lett.*, **32**, L15701, doi:10.1029/2005GL023110.
- Walker, G. T. (1924), Correlation in seasonal variations of weather. IV: A further study of world weather, *Mem. Indian Meteorol. Dep.*, **24**, 275–332.
- Watanabe, M. (2004), Asian jet waveguide and a downstream extension of the North Atlantic Oscillation, *J. Clim.*, **17**, 4674–4691.
- Webster, P. J., and S. Yang (1992), Monsoon and ENSO—Selectively interactive systems, *Q. J. R. Meteorol. Soc.*, **118**, 877–926.

Webster, P. J., V. O. Magaña, T. N. Palmer, J. Shukla, R. A. Tomas, M. Yanai, and T. Yasunari (1998), Monsoons: Processes, predictability and the prospects for prediction, *J. Geophys. Res.*, *103*, 14,451–14,510.

Yanai, M., and C. Li (1994), Mechanism of heating and the boundary layer over the Tibetan Plateau, *Mon. Weather Rev.*, *122*, 305–323.

Yanai, M., C. Li, and Z. Song (1992), Seasonal heating of the Tibetan Plateau and its effects on the evolution of the Asian summer monsoon, *J. Meteorol. Soc. Jpn.*, *65*, 81–102.

---

J. Shaman, College of Oceanic and Atmospheric Sciences, Oregon State University, Corvallis, OR 97331-5503, USA. (jshaman@coas.oregonstate.edu)

E. Tziperman, Department of Earth and Planetary Sciences, Harvard University, Cambridge, MA 02138, USA.